



Relation between Velocity and Pressure in circular and Non-Circular Shape Duct for Local Exhaust Ventilation (LEV) System

M. Farid Sies¹, M. Zikrul M. Sharif¹, Maznan Ismon¹, Hanis Zakaria¹, M. Nur Hidayat Mat², M. Amran Madlan^{3*}

¹Mechanical Engineering Department, Faculty of Mechanical and Manufacturing Engineering, Universiti Tun Hussein Onn Malaysia (UTHM), MALAYSIA

²School of Mechanical Engineering, Faculty of Engineering, Universiti Teknologi Malaysia (UTM), MALAYSIA

³Faculty of Engineering, Universiti Malaysia Sabah (UMS), MALAYSIA

*Corresponding author

DOI: <https://doi.org/10.30880/jamea.2022.03.01.003>

Received 24 February 2022; Accepted 21 April 2022; Available online 20 July 2022

Abstract: Local exhaust ventilation (LEV) is used to isolate contaminants from the source. It is vital to ensure good air quality, particularly for employees exposed to hazardous gases such as high-temperature factories and kitchens where food is cooked. This simulation explores how a particular cross-sectional duct structure influences the ventilation device's velocity distribution and pressure decrease. The system's design consists of a collecting hood, 90° bends, 45° bends, and a straight pipe. Three models use the same volume around the unit. There are circular (Model A), square (Model B), and rectangular (Model C). This study is carried out using Computational Fluid Dynamic (CFD). The simulation shows the behaviour of the airflow from the inlet to the exit in all three models. Model A is the most preferable of the results produced because the velocity distribution in this circular line is even and more balanced. The average velocity of the model A device is a mean of 2.80m/s, and the lowest mild pressure is -76.74 Pa. Changes in the path of the system's flow creates eddy and disturbance to the system's flow. Higher pressure to sustain the optimal flow speed will increase energy consumption and help more robust preliminary designs for local exhaust ventilation.

Keywords: Local exhaust ventilation, ducting, velocity, pressure, computational fluid dynamic

1. Introduction

This paper uses computational fluid dynamics software to investigate the velocity distribution and pressure drop in circular and non-circular ducting. A ventilation system's selection is based on interior air quality, heating and cooling loads, preference for outside environments, cost, and layout. A practical, well-designed ventilation system is the answer to the problem of worker safety. A ventilation system aims to control odors, humidity, and other unwelcome environmental elements (American Conference of Governmental Industrial Hygienists, 1998). Clean air is brought into a building and circulated throughout the building, while contaminated air is removed through ventilation.

Indoor air quality is critical for workers, particularly those who work in welding shops. For example, welding shops require enough ventilation to remove fumes generated by welding operations from their work areas. Welding fumes can harm human health if the air is not adequately ventilated. The optimal ducting cross-sectional shapes will increase local exhaust ventilation efficiency and energy consumption. Circular and non-circular ducting are common in local exhaust ventilation systems because they slow down airflow and cause losses inefficiency. This simulation aims to determine whether a changing cross-sectional ducting shape would alter velocity distribution and pressure drop.

A well-designed LEV system should have minimal investment and operating expenses and excellent ventilation efficiency. Ducts shapes come in various forms, including circular, rectangular, and oval. Xu and Wang (2020) mention that fluid flows in circular ducts have received more attention in the literature than those in non-circular ducts [1]. Zhang (2021) investigated whether a radial jet at the outside edge of a circular exhaust hood may minimize velocity attenuation in front of the hood. The velocity distribution, particularly the centerline velocity, is crucial for practical design and usage [2]. Air conditioning systems employ a variety of ducts, including circular, rectangular, oval, and other shapes. Circular ducts have traditionally been used in systems because of their benefits, including efficiently transporting flowing air with less friction, more accessible and faster installation, less noise, and a lower initial cost. On the other hand, round ducts require more height than rectangular or square ducts; thus, rectangular or square ducts are preferable in many HVAC (Heating, Ventilation, and Air Conditioning) applications when space is limited [3]. Pressure loss and velocity are two aspects of air system balance, which are concerned with duct sizing during the design phase and testing, modifying, and balancing after installation.

Pressure losses through duct fittings such as dampers, sensors, bends, transition pieces, duct corners, branches, and splitter attenuators are critical in air-delivery duct systems to compensate for the pressure differential caused by fans [4]. Therefore, it is vital to accurately forecast the pressure losses in each duct fitting during the design phase, which might ultimately lead to significant savings in the original investment and the operational costs of duct systems [5][6][7]. Pressure is classified into four categories. There are four types of pressure: static pressure, dynamic pressure, total pressure, and absolute pressure. Potential pressure exerted in all directions by air at rest is known as "static pressure." As long as the static pressure is positive or negative, the duct expands or shrinks. As a rule, static pressure has a positive or negative sign depending on whether it is greater or lower than atmospheric pressure. The pressure created by the speed of air flowing in the flow direction is known as dynamic pressure, or velocity pressure. The total pressure is the amount of pressure that causes an air movement. The total pressure consists of two components: static and dynamic pressure. Air handling systems are built with a specified total pressure to allow optimal fan sizing [8][9].

The ducting or the piping characteristics determine a fan's performance in a duct system. For example, when a single fan or blower is positioned in two distinct locations, it will produce different flow rates and heads. Therefore, before fan selection, the typical behavior of the ducting system on which the fans are put must be identified [10][11]. The Darcy-Weisbach relation is a fundamental equation for determining the probability of a specific loss [12][13]. It may be expressed as:

$$H_L = f \frac{L V^2}{D 2g} \quad (1)$$

H_L denotes pressure loss in this relationship, and L indicates pipe length (m). D denotes internal pipe diameter (m), V denotes the average flow velocity (Flow rate/Pipe or duct Cross Section) in m/s, f represents friction coefficient, and g indicates a gravitational acceleration (m/s^2). The above equation can be written as:

$$\Delta P = f \rho \frac{L V^2}{D 2g} \quad (2)$$

where P is the loss of pressure, and ρ is the density of the liquid. The Darcy equation can be applied for any flow regime, laminar, or turbulent. The pressure loss in pipelines or duct lines with constant diameter and liquids with constant velocity and density can be calculated using equation (2) [13]–[15].

The exhaust hood must create enough capture velocity at the pollution source to withstand the escape velocity of pollutants to catch pollutants efficiently. According to previous research on the flow fields of exhaust hoods, the suction air for exhaust hoods is taken in from all hemispherical directions, resulting in an abrupt decrease of the suction velocity in front of the hood as the distance from the hood increases. Earlier research on the flow fields of exhaust hoods showed that suction air is sucked in from all hemispherical directions, resulting in a rapid decrease of the suction velocity in front of the hood with distance from it [16]–[18].

However, pressure drop and velocity are critical parameters in the duct system. Haque (2021) mentions that non-circular ducts have the advantage of reduced pressure drop and the disadvantage of low Heat Transfer Coefficient (HTC) compared to the circular duct. This research aimed to investigate the features of nanofluid flow and duct form to improve the heat transfer coefficient and lower the pressure drop by utilizing different nanoparticle concentrations [4][19][20]. Logachev (2018) conducted a computational and experimental analysis of the velocity field in the region impacted by a circular exhaust duct based on a survey of distinct airflow patterns at the entrance of circular exhaust hoods. He discovered that airflow velocity distribution patterns make choosing the most efficient exhaust duct design for reducing pollutant removal costs easier [21]–[23].

Ahmimache and Fénot [24] also observed that velocity measurement and flow structure characterization on impinging jets have yet to be accomplished. Therefore, they did the aerodynamic and thermal experiments on a single line of seven jets that came out of a pipe and hit a plate at a low Reynolds number. Heat transfer rates were determined to predominantly depend on the injection Reynolds number, injection-to-plate distance, and center-to-center spacing and relatively modest compared to a fully formed jet [25]–[27].

This paper uses computational fluid dynamics (CFD) to look at the velocity distribution and pressure drop in circular and non-circular ducting. It was done by comparing cross-section velocity and pressure drop profiles with CFD flow simulations in various duct shapes. In summary, the findings may aid in developing high-efficiency ventilation systems and reducing industrial building energy use.

2. Methodology

2.1 Model

The numerical analysis of single-phase flow in this system was performed. Ansys fluent provides a solution to the k-epsilon with associated velocity and pressure drop. The design of the LEV device relates to previous research that is acceptable for small-scale applications. The ventilation system approach is based on the American Conference of Governmental Industrial Hygienists (ACGIH) guidelines, which direct a proper local exhaust system appropriate for suctioning welding fumes. Figures 1 (a) and 1(b) show LEV device illustrations. The LEV device comprises a variety of elements. Capture Hood, Duct Device, 45-degree elbow, and 90-degree elbow are the critical parts of LEV. Figure 1 (b) shows that take the data from point number (1) until (12). This analysis has three models: a circular, square, and rectangular cross-section structure, as shown in Figure (1a) and Figure 2. In addition, there are three models, model A, model B, and model C. Each model must be optimized to ensure that the simulation runs more efficiently and effectively with three different geometric model designs, including model size and shape.

2.2 Fluid Flow Equation

In a steady or turbulent flow field, the continuity and momentum for incompressible, time-dependent, and viscous fluids are represented as follows [19][28][13]:

Continuity equation:

$$\frac{\partial u}{\partial x} + \frac{\partial v}{\partial y} + \frac{\partial w}{\partial z} = 0 \quad (3)$$

Momentum equation:

$$\rho_{nf} \left(u \frac{\partial u}{\partial x} + v \frac{\partial u}{\partial y} + w \frac{\partial u}{\partial z} \right) = -\frac{\partial p}{\partial x} + \mu_{nf} + \left(u \frac{\partial^2 u}{\partial x^2} + v \frac{\partial^2 u}{\partial y^2} + w \frac{\partial^2 u}{\partial z^2} \right) \quad (4)$$

$$\rho_{nf} \left(u \frac{\partial v}{\partial x} + v \frac{\partial v}{\partial y} + w \frac{\partial v}{\partial z} \right) = -\frac{\partial p}{\partial y} + \mu_{nf} + \left(u \frac{\partial^2 v}{\partial x^2} + v \frac{\partial^2 v}{\partial y^2} + w \frac{\partial^2 v}{\partial z^2} \right) \quad (5)$$

$$\rho_{nf} \left(u \frac{\partial w}{\partial x} + v \frac{\partial w}{\partial y} + w \frac{\partial w}{\partial z} \right) = -\frac{\partial p}{\partial z} + \mu_{nf} + \left(u \frac{\partial^2 w}{\partial x^2} + v \frac{\partial^2 w}{\partial y^2} + w \frac{\partial^2 w}{\partial z^2} \right) \quad (6)$$

There are three components of velocity in each of the three dimensions: u , v , and w . P is the pressure, μ is dynamic viscosity, and ρ is the density.

2.3 Meshing

Mesh creation in CFD is critical for engineering simulations because it is the model's foundation. In addition, the mesh impacts the simulation's accuracy, convergence, and speed. Skewness and orthogonal quality are two metrics used to assess mesh performance. Hence, the accuracy of the results, the measurement's efficiency, and the required quality, as seen in Table 1. Table 2 compared the three models in volume, percentage difference with model A, element size, node number, elements, skewness, orthogonal quality, and quality. Model A is the second smallest volume with the highest node and element. It is also the smallest skewness and has many orthogonal qualities compared to models B and C. However, model A has good quality compared to models B and C.

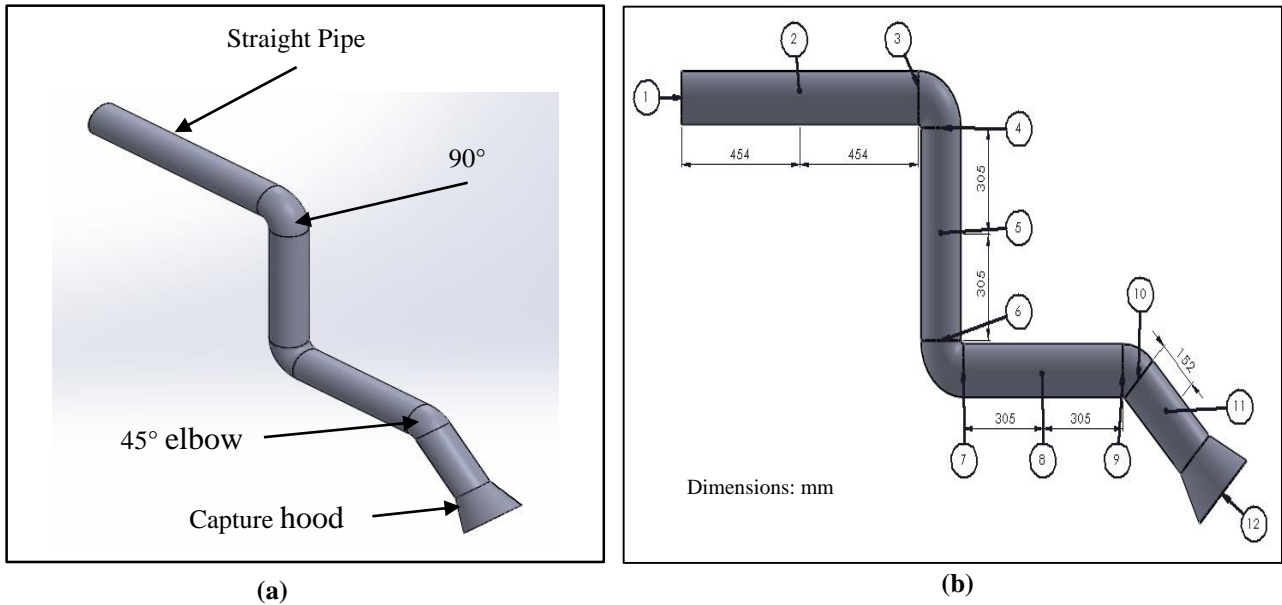


Fig. 1 - (a) Circular ducting model A and (b)The point (1-12) on model A to take the reading.

Table 1 - Mesh metrics spectrum [29]

Skewness mesh metrics spectrum					
Excellent	Very good	Good	Acceptable	Bad	Unacceptable
0-0.25	0.25-0.50	0.50-0.80	0.80-0.94	0.95-0.97	0.98-1.00
Orthogonal Quality mesh metrics spectrum					
Unacceptable	Bad	Acceptable	Good	Very good	Excellent
0-0.001	0.001-0.14	0.15-0.20	0.20-0.69	0.70-0.95	0.95-1.00

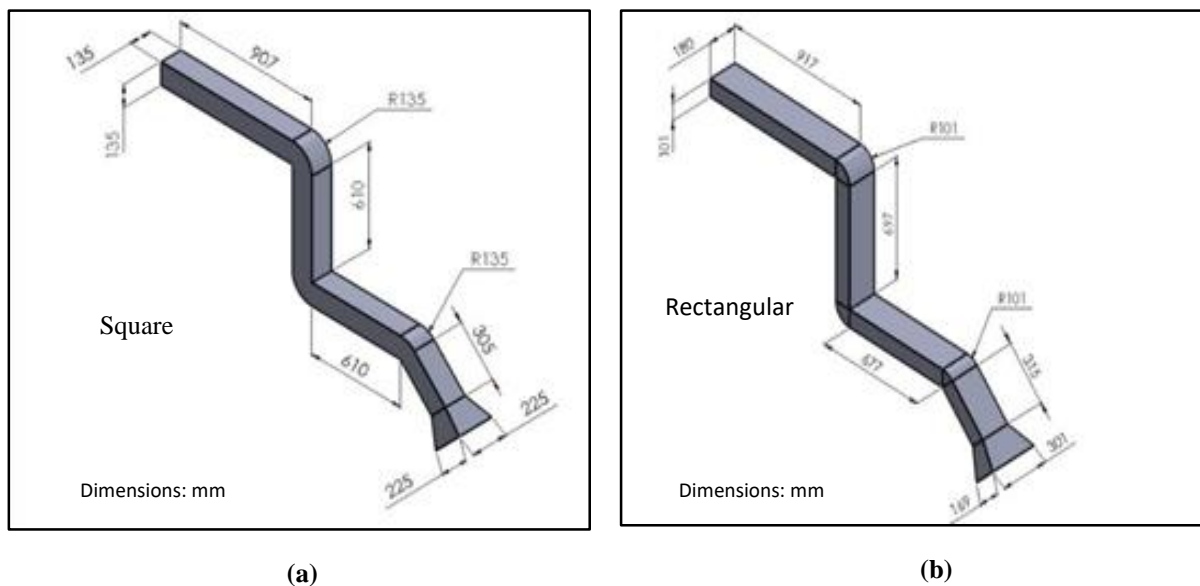


Fig. 2 - (a) Geometry Model B; (b) Geometry Model C

Table 2 - Result of meshing for model A, B, and C

Model	Volume (m ³)	% Diff. with Model A	Element Size	Node	Element	Skewness	Orthogonal Quality	Quality
A	0.0556	0 %	0.0134	31138	152762	0.79	0.21	Good
B	0.0542	2 %	0.0134	28020	136785	0.84	0.16	Acceptable
C	0.0563	1 %	0.0134	28120	136111	0.84	0.16	Acceptable

2.4 Parameter and Boundary Conditions

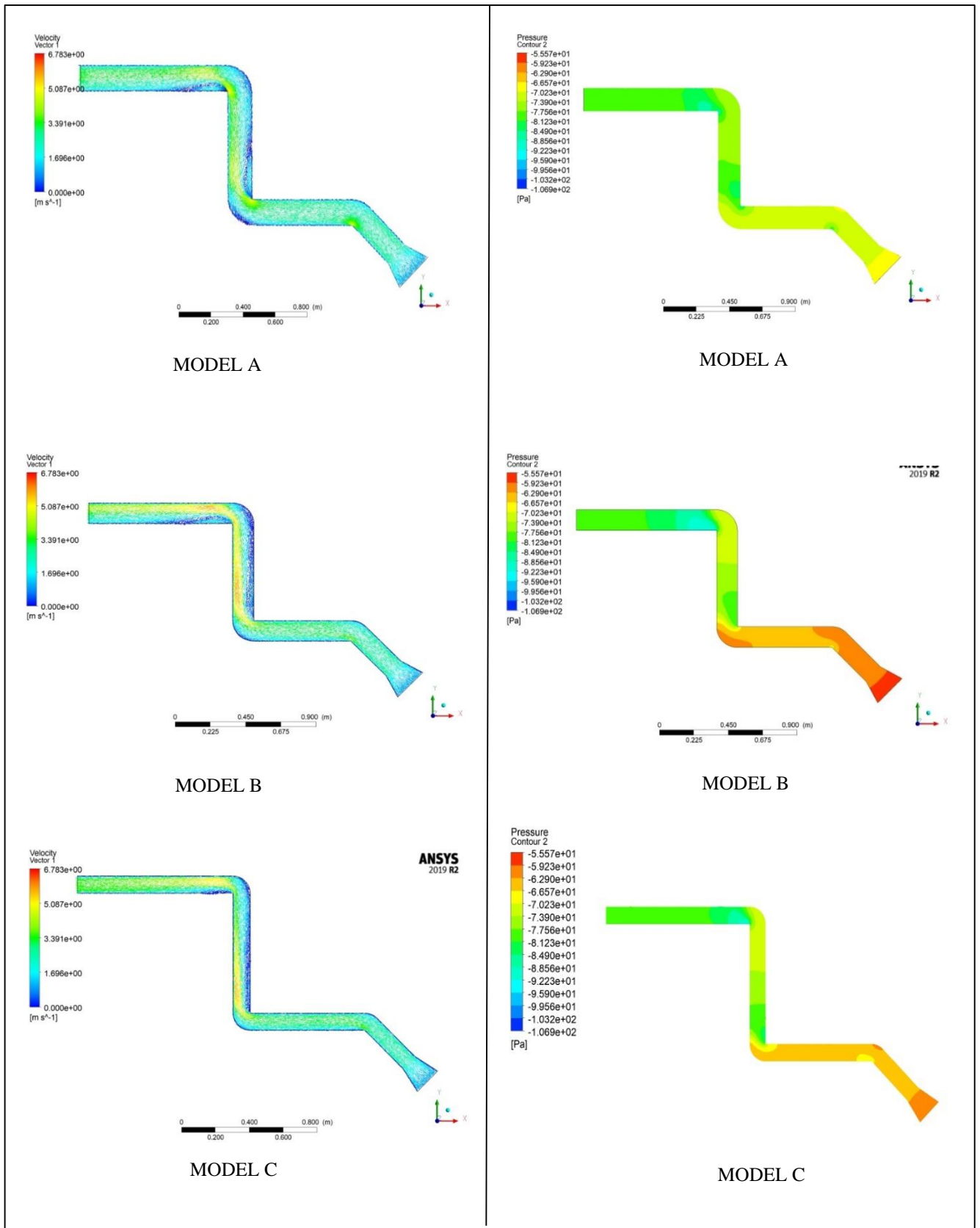
The simulation equations depend on the parameters and limit conditions at this stage. For example, the average gas welding speed should be between 0.5 and 1.0 m/s. The airflow performance in the simulated ducting system was evaluated using the commercial programmed ANSYS Fluent. Table 3 contains the parameter and boundary conditions. In this study, five parameter sources were employed to model the airflow generated by the blower. Use the coupled solution method and k-epsilon turbulent model with one (1) m/s velocity magnitude, 5 % turbulent intensity, and ten (10) turbulent viscosity ratios at the inlets. The exhaust outlet used a pressure outlet (-80 Pa) with static backflow pressure. We used a stationary wall, No-slip shear condition, and standard wall roughness for the wall application. At the working fluid, air density is 1.169 kg/m³ and 1.79E-05 m²/s viscosity.

Table 3 - The parameter and boundary condition

Parameter	Viscous	k-epsilon (2 eqn)
Inlet	Type of boundary	Velocity -Inlet
	Velocity magnitude	1 m/s
	Turbulent intensity	5%
	Turbulent Viscosity Ratio	10
Outlet	Type of boundary	Pressure-outlet
	Gauge Pressure	-80 Pa
	Backflow Pressure Specification	Static Pressure
Wall	Wall motion	Stationary Wall
	Shear Condition	No-slip
	Wall Roughness	Standard
Working Fluid	Type	Air
	Density	1.169 kg/m ³
	Viscosity	1.79E-05 m ² /s
Solution Method	Pressure-Velocity Coupling	Coupled

3. Results

Figure 3 presents the result obtains for the development of velocity and pressure in the ducting with various design (Model A, B and C). In order to determine the velocity and pressure contour of the ducting are showed in Fig. 3(a) and 3(b). The distribution of pressure that forms in a system varies. It is critical to know the pressure to calculate the system's loss. Model A has a maximum inlet pressure of -68.07 Pa, while models B and C have a pressure of -57.56 Pa and -60.05 Pa, respectively. The outer wall of the 45° and 90° bends has a higher pressure region, while the inner wall has lower pressure. Therefore, model A has a smaller low-pressure area at the inner wall of 45° and 90° bends than models B and C. There is a difference in pressure between the outer and inner walls of the bend due to differences in inflow velocity. Model A used low pressure to keep the air flowing because there is less pressure loss in the system than in models B and C. Before the first 90° bend from the inlet, the pressure is higher. After the bend, the pressure goes down. The same phenomenon occurs at the second 90° bend from the inlet, demonstrating that pressure drop occurs at all the system's fittings. The average system pressure for models A, B, and C is -76.74 Pa, -71.24 Pa, and -72.13 Pa, respectively.



(a) Velocity contour

(b) Pressure contour

Fig. 3 - Contour intensity development for different models

Figure 4 shows each model's velocity and average velocity from point number one (1) to point number twelve (12). Overall, model A illustrates a higher average speed compared with other models. Then, the average velocity value for model A is 2.97 m/s, followed by model B, which is 2.77 m/s, and finally, model C is 2.72 m/s. However, the three model results had some fluctuations. Although model C is the smallest average speed value, it has the highest volume compared to models A and B. Point number four (4) for model A has the highest velocity value than another point of approximately 3.93 m/s. Then, it decreases to 2.84 m/s at point number Five (5). However, it increases again at points six (6) and seven (7).

The duct or pipe system is susceptible to pressure drops. Figure 4 illustrates the pressure drop and average pressure drop for various shapes. It can be seen that the number of pressure drops in model A is -80.00 Pascal in point one (1) to -68.07 Pascal in point twelve (12), with a minor average of -76.74 pa compared with other models. Thus, the number of model pressure drops is a relative decrease for all models, starting at point four (4) until point twelve (12). However, model B has the most significant average value compared with other models because it has the smallest value of ducting volume. Overall, Bernoulli's formula summarizes the relationship between pressure and velocity as inversely proportional. As pressure grows, the velocity decreases, resulting in the algebraic total of potential energy, kinetic energy, and pressure being constant as pressure increases.

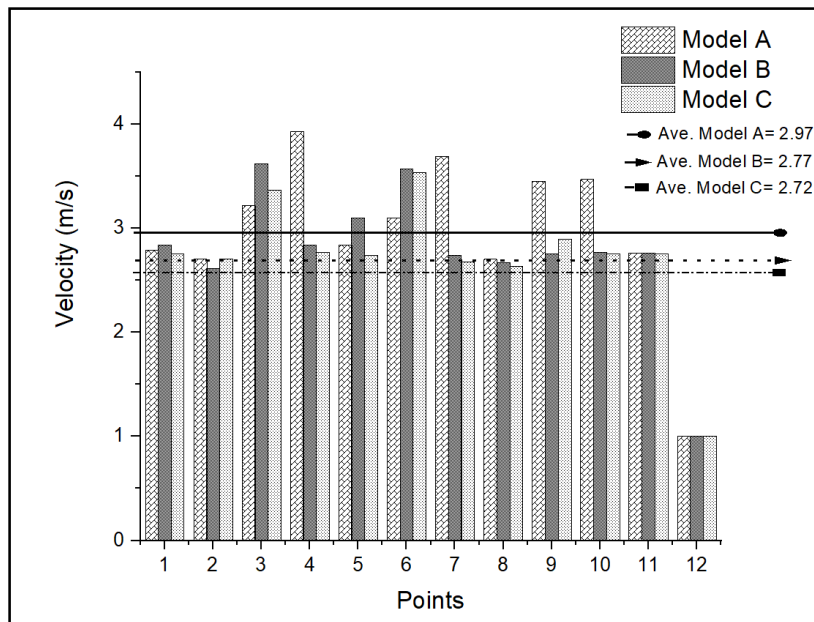


Fig. 4 - Velocity and average velocity from the 12 points on the Duct system for models A, B, and C

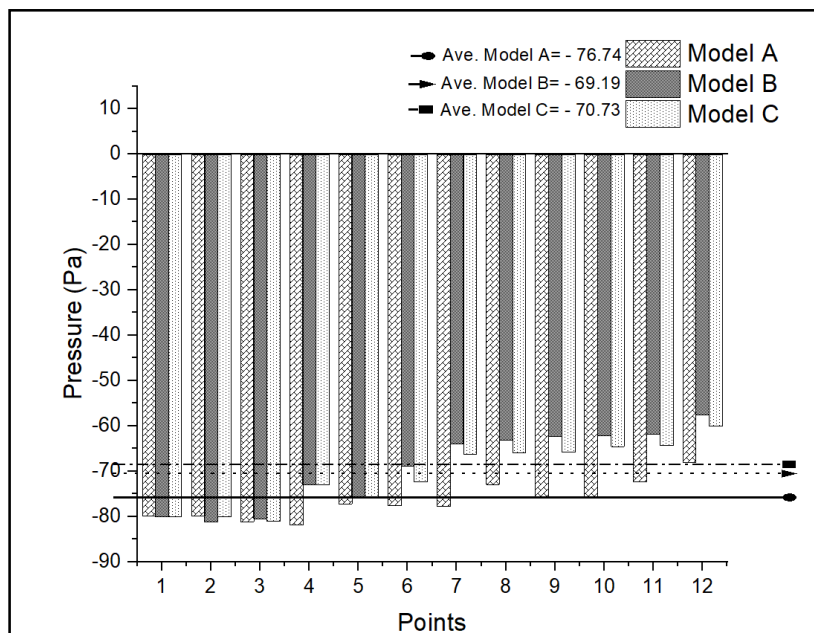


Fig. 5 - Pressure drop and average pressure drop from the 12 points on the Duct system for models A, B, and C

4. Discussions

This research evaluated the velocity and pressure of circular and non-circular ducting in the twelve (12) locations measured based on the information collected from this study. Unfortunately, due to the LEV system's small scale, we cannot get a more in-depth result. On the other hand, this finding may aid researchers in enhancing the ventilation system's overall efficiency by determining the optimum cross-sectional ducting shape and other essential characteristics. Circular ducting improves airflow resistance, friction, and efficiency. It's also easier to put up, works better in systems with medium to high pressure, and costs less to set up initially than other options. For this reason, the LEV system is more efficient since it has less noise pollution generated by these ducts than with different kinds of ducts [5].

The circular or round duct is easier to construct and utilize standard components such as fittings. As a result, it contributes to reduced initial cost and more pressure structurally than a non-circular duct. Non-circular ducts need more material and components like bolts, rivets, support beams. The hydraulic diameter (D.H.) for a circular duct is better than a rectangular duct because a circular duct requires less material. Then, the measurement point for air volume is smaller than in a non-circular duct. Additionally, a balanced duct system requires less commissioning than a non-circular duct. The circular duct substantially reduces low-frequency noise in the space and minimizes noise-canceling equipment requirements [2][30].

Since the circular duct lowers air leakage, it will become increasingly popular. Air leakage is a significant cause of wasted energy, decreased efficiency, and poor indoor air quality in commercial HVAC systems. Because spiral ductwork has fewer duct-to-duct connections (or joints) than rectangular ductwork, it has a leakage rate of less than 1% when engineered and installed appropriately. Finally, because of its silence and big size, a rectangular duct is chosen for many high-flow and large-size duct system components, such as natural air suction (inlets) and air treatment devices (outlets).

5. Conclusion

This study uses simulation to analyze the pressure drop and velocity distribution in various ducting shapes using three (3) models (Model A, B, and C). Each model contains a straight pipe, 45-degree bend, and 90-degree bend, as well as a capturing hood with the same volume throughout the system. The most efficient way to carry air is through circular ducts (Model A). They need less material than non-circular ducts to handle the same air volume. Circular ducting in Model A is preferable because the velocity distribution in this circular ducting is more even and balanced since it is more miniature eddy. The pressure distribution in model A is more even, and less pressure drop occurs because it does not require high pressure to sustain the airflow in the system at the desired velocity. The average speed throughout the model A design is the highest, with the intermediate pressure lowest compared to models B and C. The changes in the direction of the flow in the system form eddy and disturbance to the system's flow. The relation between velocity and pressure can be observed when the speed is inversely proportional to the pressure, which shows that if the pressure is low, the higher the velocity. Model A uses circular ducting, making it the best design and performance for these studies. In addition, the pressure drop is less, and the velocity of airflow is evenly distributed. Hence, it is a suitable design because it can save energy consumption. In conclusion, the LEV system's operation recommendations include adding the air filter, fan, and stack. The lowest suction pressure at the design's output by comparing the different suction pressure magnitudes and achieving the most downward force necessary to maintain an airflow satisfies DOSH Malaysia's standard requirements.

Acknowledgment

This research was supported by Universiti Tun Hussein Onn Malaysia (UTHM) through TIER 1 (Vot H923).

References

- [1] H. Xu, S. Wang, and M. Zhao, "Oscillatory flow of second grade fluid in a straight rectangular duct," *J. Nonnewton. Fluid Mech.*, vol. 279, no. 104245. January, 2020.
- [2] J. Zhang et al., "Experimental and numerical study of the effect of perimeter jet enhancement on the capture velocity of a rectangular exhaust hood," *J. Build. Eng.*, vol. 33, no. 101652. April 2020, 2021.
- [3] H. Park and C. K. Bach, "Performance characterization of air mixing devices for square ducts," *Appl. Therm. Eng.*, vol. 199, no. 117495. May, p. 117495, 2021.
- [4] M. E. Haque, M. S. Hossain, and H. M. Ali, "Laminar forced convection heat transfer of nanofluids inside non-circular ducts: A review," *Powder Technol.*, vol. 378, pp. 808–830, 2021.
- [5] Z. T. Ai and C. M. Mak, "Pressure losses across multiple fittings in ventilation ducts," *Sci. World J.*, vol. 2013, 2013.
- [6] O. A. Elsamni, A. A. Abbasy, and O. A. El-Masry, "Developing laminar flow in curved semi-circular ducts," *Alexandria Eng. J.*, vol. 58, no. 1, pp. 1–8, 2019.
- [7] K. Peszynski and V. Tesař, "Algebraic model of turbulent flow in ducts of rectangular cross-section with rounded corners," *Flow Meas. Instrum.*, vol. 75, no. 101790. July, 2020.
- [8] H.A.Shah, "Design & Proportional Computational Assessment Between a Conventional and Circular Duct System," *J. Emerg. Technol. Innov. Res.*, no.7. August, 2019.

- [9] L. Czetany, Z. Szantho, and P. Lang, "Rectangular supply ducts with varying cross section providing uniform air distribution," *Appl. Therm. Eng.*, vol. 115, pp. 141–151, 2017.
- [10] H. B. Nourbakhsh, S. A., Jaumotte, B. A., Hirsch, C., & Parizi, "Pipeline Calculations 7.1," in *Turbopumps and Pumping Systems*, vol. 82, 2007, pp. 82–97.
- [11] Kast, W., (Revised by Hermann Nirschl), Gaddis, E. S., Wirth, K.-E. & Stichlmair, J. (2010). *L1 Pressure Drop in Single Phase Flow*. In *VDI Heat Atlas* (pp. 1053-1116) . Springer Berlin Heidelberg . ISBN: 978-3-540-77876-9.
- [12] R. T. Renata, F. F. S. Pereira, T. B. G. da Silva, E. R. Castro, and J. C. C. Saad, "The performance of explicit formulas for determining the darcyweisbach friction factor," *Eng. Agric.*, vol. 40, no. 2, pp. 258–265, 2020.
- [13] A. Ramadhan Al-Obaidi and I. Chaer, "Study of the flow characteristics, pressure drop and augmentation of heat performance in a horizontal pipe with and without twisted tape inserts," *Case Stud. Therm. Eng.*, vol. 25, no. 100964, October 2020.
- [14] Y. Baghernejad, E. Hajidavalloo, S. M. Hashem Zadeh, and M. Behbahani-Nejad, "Effect of pipe rotation on flow pattern and pressure drop of horizontal two-phase flow," *Int. J. Multiph. Flow*, vol. 111, pp. 101–111, 2019.
- [15] W. Jia and J. Yan, "Pressure drop characteristics and minimum pressure drop velocity for pneumatic conveying of polyacrylamide in a horizontal pipe with bends at both ends," *Powder Technol.*, vol. 372, pp. 192–203, 2020.
- [16] L. Benia, "Experimental Evaluation of the Velocity Fields for Local Exhaust Hoods with Circular and Rectangular Openings," *Build. Environ.*, vol. 31, no. 5, 1996.
- [17] B. Fletcher, "Effect of flanges on the velocity in front of exhaust ventilation hoods," *Ann. Occup. Hyg.*, vol. 21, no. 3, pp. 265–269, 1978.
- [18] B. Fletcher and A. E. Johnson, "Velocity profiles around hoods and slots and the effects of an adjacent plane," *Ann. Occup. Hyg.*, vol. 25, no. 4, pp. 365–372, 1982.
- [19] X. Li and S. Wang, "Flow field and pressure loss analysis of junction and its structure optimization of aircraft hydraulic pipe system," *Chinese J. Aeronaut.*, vol. 26, no. 4, pp. 1080–1092, 2013.
- [20] S. Li, W. Huai, N. S. Cheng, and G. Coco, "Prediction of mean turbulent flow velocity in a permeable-walled pipe," *J. Hydrol.*, vol. 573, no. 135305184, March, pp. 648–660, 2019.
- [21] K. I. Logachev, A. M. Ziganshin, O. A. Averkova, and A. K. Logachev, "A survey of separated airflow patterns at inlet of circular exhaust hoods," *Energy Build.*, vol. 173, pp. 58–70, 2018.
- [22] M. G. L. C. Loomans, I. M. De Visser, J. G. H. Loogman, and H. S. M. Kort, "Alternative ventilation system for operating theaters: Parameter study and full-scale assessment of the performance of a local ventilation system," *Build. Environ.*, vol. 102, pp. 26–38, 2016.
- [23] S.-H. Jeong, H.-M. Kwon, S.-J. Ahn, and J.-H. Yang, "A Study on the Improvement of Ventilation Rate Using Air-flow Inducing Local Exhaust Ventilation System," *J. Asian Archit. Build. Eng.*, vol. 15, no. 1, pp. 119–126, 2016.
- [24] Y. Ahmimache, M. Fénot, F. Plourde, and L. Descamps, "Heat transfer and flow velocity study of a row of jets emerging from a perforated pipe at a low Reynolds number," *Int. J. Heat Mass Transf.*, vol. 183, p. 122067, 2022.
- [25] N. Furuichi and M. Ono, "Static pressure measurement error for wall taps with high Reynolds number turbulent pipe flow," *Flow Meas. Instrum.*, vol. 79, no. 101962, p. 101962, 2021.
- [26] T. Xia, Y. Bian, L. Zhang, and C. Chen, "Relationship between pressure drop and face velocity for electrospun nanofiber filters," *Energy Build.*, vol. 158, pp. 987–999, 2018.
- [27] G. Takacs et al., "Determining velocity and friction factor for turbulent flow in smooth tubes," *Energy Build.*, vol. 40, no. 2, pp. 258–265, 2020.
- [28] S. Kumar, M. Kumar, S. Samanta, M. Ukamanal, A. R. Pradhan, and S. B. Prasad, "Simulations of water flow in a horizontal and 900 pipe bend," *Mater. Today Proc.*, no. (2). 2022.
- [29] M. Ozen, "Meshing workshop," Sunnyvale, California, 2014.
- [30] P. C. Raynor et al., "Comparison of stainless and mild steel welding fumes in generation of reactive oxygen species," *Part. Fibre Toxicol.*, vol. 7, no. 1, pp. 1–13, 2015.